

Visualization of femorotibial contact in total knee arthroplasty using X-ray fluoroscopy

Takaharu Yamazaki^{a,*}, Tetsu Watanabe^b, Yoshikazu Nakajima^a, Kazuomi Sugamoto^b, Tetsuya Tomita^b, Daisuke Maeda^c, Wataru Sahara^b, Hideki Yoshikawa^b, Shinichi Tamura^a

^a Department of Medical Robotics and Image Sciences, Osaka University, Graduate School of Medicine, 2-2 Yamadaoka, Suita, Osaka 565-0871, Japan

^b Department of Orthopaedics, Osaka University, Graduate School of Medicine, 2-2 Yamadaoka, Suita, Osaka 565-0871, Japan

^c Department of Radiology, Osaka University Hospital, 2-2 Yamadaoka, Suita, Osaka 565-0871, Japan

Received 15 September 2003; accepted 17 November 2003

Abstract

The purpose of this study was to build a visualization technique of the femorotibial contact in fixed-bearing total knee arthroplasty (TKA) using X-ray fluoroscopy, and to apply this technique to a TKA patient during dynamic motion. In vivo kinematics of the metallic knee implant was determined using a 2D/3D registration technique, which uses computer assisted design (CAD) model of the implant to estimate the 3D pose of radiopaque metallic femoral and tibial components from a single-plane fluoroscopic image. In fixed-bearing TKA, a 3D pose of radiolucent tibial polyethylene insert can be determined from the estimated pose of the tibial component. To visualize femorotibial contact, the proximity between surfaces of femoral component and tibial insert was calculated, and mapped onto the insert surface model. For the clinical application, dynamic states of contact on the tibial insert were observed including axial rotation and unilateral loading during knee flexion, and post-cam contact of posterior stabilized TKA. The present technique provided us new information and enabled us to better understand the relationship between in vivo knee kinematics and articular shape of the implant.

© 2003 Elsevier Ireland Ltd. All rights reserved.

Keywords: Visualization; Femorotibial contact; Total knee arthroplasty; Kinematics; X-ray fluoroscopy

1. Introduction

Total knee arthroplasty (TKA) is an effective treatment for functional disability and arthritic knees in which articular cartilage is damaged. TKA implants generally consist of metallic femoral and tibial components and a polyethylene bearing insert between them. The polyethylene insert replaces the damaged cartilage of the tibial plateau and provides a low-friction surface for the metallic implant component. Knee kinematics and the durability after TKA depend on the variable articular shapes of the femoral component and tibial insert. Wear in the polyethylene tibial insert, which is one of the reasons for revision surgery, has been regarded to be the result of high contact stress on the articular surface as well as from sliding and skidding motions [1,2].

Knowledge of joint contact and its area after TKA could not only provide kinematic information dependent on articu-

lar shape but also assist in improving the design of implants that include tibial polyethylene insert. In previous studies, joint contact in TKA was evaluated using a finite element model [3] and pressure sensitive film or digital tactile sensor [4,5]. These methods have provided information regarding joint contact under static *in vitro* conditions.

Recently, several laboratories have reported dynamic *in vivo* kinematics of TKA prosthesis using 2D/3D registration technique [6–8], which determine the spatial position and orientation for metallic femoral and tibial component from X-ray fluoroscopy and computer-assisted design (CAD) model of the implant. These studies could provide information regarding the relative movement of radiopaque femoral and tibial components, but could not provide information of radiolucent polyethylene insert. Therefore, it was difficult to obtain the knowledge of actual contact between femoral component and tibial insert.

In fixed-bearing TKA, however, this insert can be taken as rigidly connected with the tibial component, so that the 3D pose of the radiolucent polyethylene insert can be determined from the estimated pose of the tibial component.

* Corresponding author. Tel.: +81-6-6879-3564;

fax: +81-6-6879-3569.

E-mail address: yamazaki@image.med.osaka-u.ac.jp (T. Yamazaki).

From 3D pose of TKA implants with tibial insert, femorotibial contact can be reproduced. The purpose of this study was to build a visualization technique of the femorotibial contact in fixed-bearing TKA using X-ray fluoroscopy, and to apply this technique to a TKA patient during dynamic motion.

2. Materials and methods

In order to assess femorotibial contact of TKA implants under dynamic in vivo conditions, we utilized a 2D/3D registration technique using X-ray fluoroscopy. This technique is able to estimate 3D pose from a known geometrical 3D object and a projected 2D silhouette image. In this study, the fixed-bearing knee implant and its 3D computer model were used. Although the tibial polyethylene insert is radiolucent and does not appear on fluoroscopic images, the 3D pose can be approximately determined from the 3D pose of the tibial component. After pose estimation of each component, the proximity between surfaces of the femoral component and tibial insert is calculated, and mapped onto the insert surface model. Thus, visualization of the femorotibial contact consists of two steps; 2D/3D registration and proximity calculation.

2.1. Conditions and requirements

Pose estimation of knee implants using X-ray fluoroscopy requires an accurate geometrical model of the implants and geometrical parameters of the X-ray imaging system. With this knowledge, a 3D pose of implants can be completely determined. The 3D geometry of a knee implant is taken from computer assisted design data of the implant (Fig. 1).

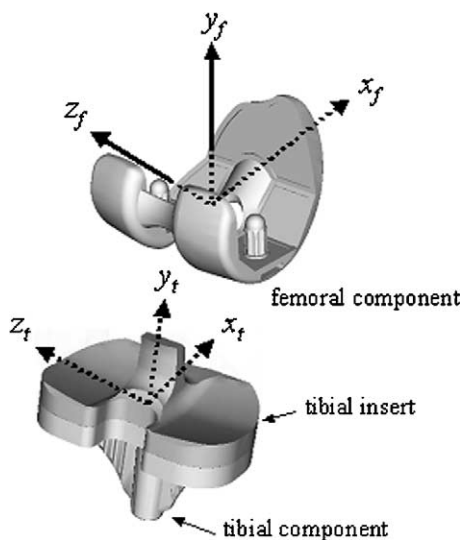


Fig. 1. Computer assisted design (CAD) data of the knee implant used. Femoral ($o_f - x_f y_f z_f$) and tibial ($o_t - x_t y_t z_t$) component coordinate systems are shown.

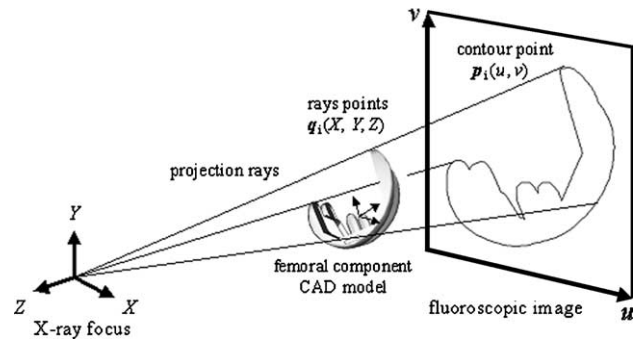


Fig. 2. Scheme of the 3D pose estimation of the model using X-ray fluoroscopy.

The parameters of the imaging system are determined using a 217-marker 3D calibration cube. First, the calibration cube is placed in the viewing area of the imaging system and X-ray images are acquired. Next, because the X-ray images exhibit significant distortion introduced by image intensifiers, images are corrected using non-linear distortion correction [9]. Finally, parameters of imaging system (principal point and principal distance) are determined from 2D data (positions of the center of projected markers) on the corrected X-ray images and the known 3D data (positions and orientation) of the calibration cube using a non-linear calibration technique [10]. The principal point is the location on the image plane where X-rays are incident perpendicularly, and principal distance is the distance from the X-ray focus to the principal point.

In vivo knee motion after TKA was recorded as a series of digital X-ray images (1024×1024 pixels; 12 bits; 7.5 frames/s) using a 12 in. digital image intensifier system (C-vision PRO-T, Shimadzu, Japan). Tests were typically performed using X-ray parameters of 70 kV, 400 mA and 1.2–2.0 ms duration, enabling nearly blur-free imaging of motion with higher per-frame exposure and image quality than in standard video-fluoroscopy.

In X-ray fluoroscopic images, metallic knee implants appear much darker than the surrounding soft tissue because of the high density of the material. Edge detection of the metallic implant is, therefore, a relatively easy image processing task. In this study, a Gaussian–Laplacian filter and threshold was applied to extract knee implant contours, and the obtained contours were utilized to estimate the 3D pose of the implant.

Table 1
Pose estimation errors of femoral component relative to tibial component

Error	Translation			Rotation		
	In-plane		Out-of-plane	Out-of-plane		In-plane
	x (mm)	y (mm)	z (mm)	x (°)	y (°)	z (°)
RMS errors	0.57	0.31	1.03	0.25	0.56	0.62
Worst errors	−0.84	−0.48	−2.09	0.46	0.84	0.80

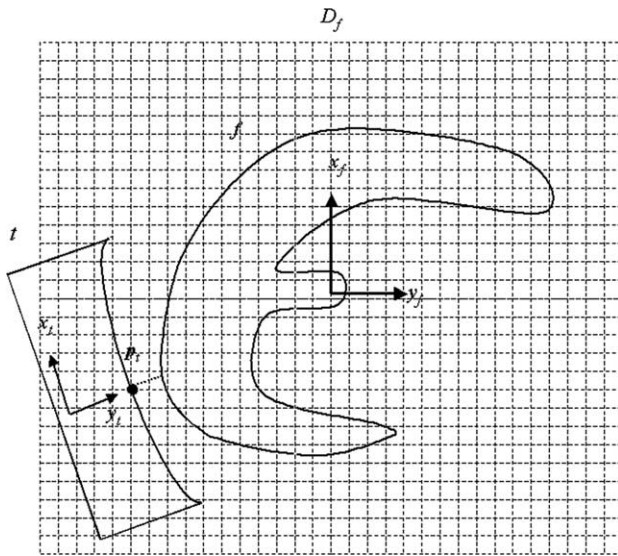


Fig. 3. 2D illustration in the medio-lateral view of a distance volume map for the femoral component. The distance from point p_i on tibial insert surface to femoral surface f is simply calculated by looking up D_f for p_i .

2.2. 2D/3D registration and the accuracy validation

The 2D/3D registration technique used was built on the contour-based registration algorithm [8]. The basic concept of the algorithm is that the 3D pose of a model can be determined by projecting rays from contour points in an image back to the X-ray focus, and noting that all of these rays are tangential to the model surface (Fig. 2). The tangent condition therefore corresponds, in practice, to the minimum distance condition between the projection rays and the model surface. Then, a cost function is defined as the sum of Euclidean distance d_i from point q_i on the projection rays (corresponding to the point p_i on the contours) to the closest point s_i on the CAD model surface. The distance d_i is given by

$$d_i = \pm |q_i - s_i|$$

where $0 \leq i < N$ and N is the number of contour points. In addition, negative values indicate rays that cross the model surface. To reduce computation time for the distance between projection rays and the model surface, a 3D distance volume map of the model was pre-computed [11]. The map stores the Euclidean distance from any point in the neighborhood of the object to the closest point on the model surface. In our study, a distance volume map with a resolution of 0.25 mm was used.

The 3D pose of the femoral and tibial component model was estimated by minimizing the sum of d_i iteratively using a non-linear optimization technique [12]. The tibial polyethylene insert, which is radiolucent and does not appear on fluoroscopic images, was assumed to be fixed on the metallic tibial component and not to undergo any deformation or movement. Hence, the 3D pose of the tibial insert was approximately determined on top of the estimated pose of tibial component.

The relative pose between the femoral component and the tibial insert (or tibial component) was finally determined by employing a three-axis Euler-angle system [13]. The pose was then denoted by six variables, three translations and three rotations.

In order to ensure the validity of 3D pose estimation of each component, the accuracy of 2D/3D registration using a single-plane fluoroscopic image was demonstrated through in vitro tests. Femoral and tibial components were installed in artificial bones, and fluoroscopic images of the artificial knee implants were taken in 10 different relative poses. From the collected images, the relative pose of the femoral component with respect to the tibial component was estimated using the 2D/3D registration technique described. Experimental accuracy was assessed by comparing these estimates with position measurements from the same knee implants obtained using an accurate 3D digitizer (Optotrak 3020: Northern Digital Inc., Canada). This digitizer is able to localize point coordinates in a 3D space using a dot probe and has an accuracy of about 0.1 mm.



Fig. 4. X-ray and CAD model images from a TKA patient during deep knee flexion. (a) Representative X-ray fluoroscopic image. (b) Image with femoral and tibial CAD models overlaid. (c) Image of virtual tibial insert model between the femoral and tibial components.



Fig. 5. Relative movement between the femoral component and the tibial component with the tibial insert. The movement is shown as the positional relationships at flexion angles of (a) 0.0°, (b) 31.9°, (c) 66.4°, (d) 87.8°, and (e) 110.7°.

Table 1 summarizes the relative pose estimation errors. The root-mean-square (RMS) errors and worst errors are given. The errors in translations and rotations were smaller than those of previous reports [8], because a higher resolution image and distance volume map was used. The accuracy was clinically sufficient for analyzing TKA kinematics.

2.3. Proximity calculation and visualization of femorotibial contact

After performing the 3D pose determinations for femoral component and tibial insert, the proximity between the CAD model surfaces of the femoral component and the tibial insert is calculated. The proximity between two surfaces is taken as the normal distance from a point on tibial insert surface to a corresponding point on femoral surface.

A geometric model of the tibial insert, which was subdivided each triangular section having a side length of 1 mm, consists of a number of triangular patches. A gravity center for each triangle patch is computed as a representative point of the patch. Thus, the normal distances from every representative point in the insert surface to every femoral surface are calculated.

In our study, distance from the representative point on insert surface to femoral surface was calculated in a simple and efficient way with the help of distance volume map of the femoral component (described in Section 2.2). As shown in Fig. 3, the femoral component has a surrounding distance volume map D_f , over which the map is sampled. Therefore, the distance from the point p_t on insert surface to femoral surface f was simply calculated by looking up D_f for p_t .

The calculated proximity was mapped onto the insert surface model by false color. The mapping was performed by

adding the areas of the triangle patches related to the representative points on the insert surface. In this study, distribution of the proximity was visualized within a range of 2.0 mm. The femorotibial contact was visualized as the region on the insert surface where the proximity is less than 0.5 mm threshold. The centroid of this region was also computed separately for both the medial and lateral surfaces as an approximation of the contact center in an attempt to evaluate the translation of that region on the tibial insert surface.

Our visualization system was implemented using a visualization tool kit [14], with all programs written in Visual C++. The system was run on an Intel Pentium III computer, 1.2 GHz, 512 Mb RAM, under Windows XP Professional edition.

3. Clinical application and results

Estimation of the femorotibial contact was performed using images taken from a TKA patient during dynamic motion, together with estimation of the relative pose of the femoral component with respect to the tibial component. The object of the study was explained to the patient, and formal consent was obtained. A time sequence of 80 fluoroscopic images was collected during deep knee flexion.

Fig. 4a–c show a representative X-ray fluoroscopic image, an image of the femoral and tibial CAD models overlaid on the X-ray image after pose estimation, and an image of the tibial insert model on the tibial model, respectively. Although the tibial insert is not appeared on the fluoroscopic image, the model was virtually visualized on top of the estimated pose of tibial component.

Table 2
Values of motion parameters of femoral component with respect to tibial component

Parameter	Knee flexion angles (°)				
	0.0	31.9	66.4	87.8	110.7
Internal (–)/external (+) rotation (°)	–0.5	1.1	8.0	14.6	10.6
Adduction (–)/abduction (+) (°)	0.1	0.9	0.7	0.5	2.2
Posterior (–)/anterior (+) translation (mm)	–6.4	–4.7	–6.2	–8.9	–14.6
Medial (–)/lateral (+) translation (mm)	–0.2	0.3	0.1	–0.5	–0.3
Proximal (–)/distal (+) translation (mm)	27.3	28.2	30.1	31.2	32.1

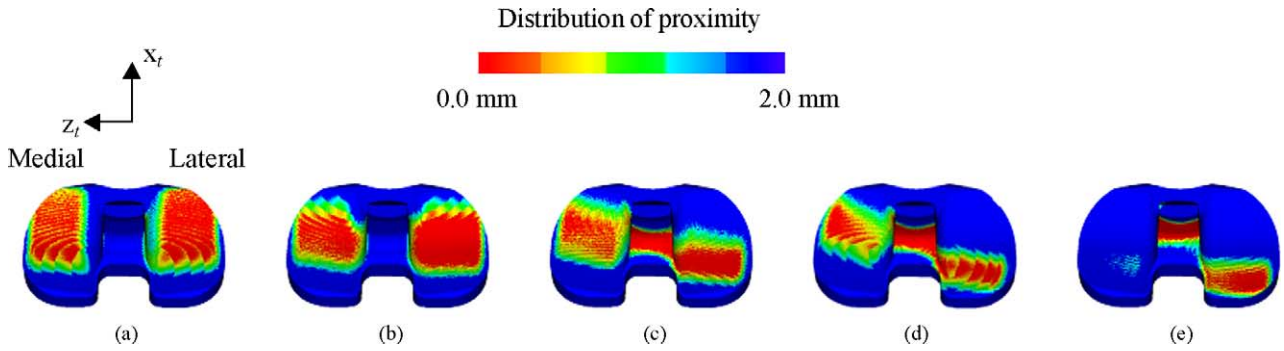


Fig. 6. Visualization of contact on tibial insert surface (proximal view) at flexion angles of (a) 0.0°, (b) 31.9°, (c) 66.4°, (d) 87.8°, and (e) 110.7°. The red area denotes where proximity is within the 0.5 mm threshold and is considered to be the virtual contact region.

Table 3

Values of virtual contact region on the medial and lateral surfaces of the tibial insert at flexion angles of (a) 0.0°, (b) 31.9°, (c) 66.4°, (d) 87.8°, and (e) 110.7°

Medial/lateral	Knee flexion angles (°)				
	0.0	31.9	66.4	87.8	110.7
Medial surface (mm ²)	295.9	283.5	176.6	137.4	0.0
Lateral surface (mm ²)	497.9	634.7	220.4	91.1	133.2

Fig. 5 shows the sequentially measured movement of the femoral component relative to the tibial component with the tibial insert in a medio-lateral view. The movement between the two components having an axis defined in Fig. 1 is shown as the positional relationships at flexion angles of 0.0, 31.9, 66.4, 87.8, and 110.7°. The values of the other motion parameters at each flexion angle are listed in Table 2.

Fig. 6 visualizes the contact on the tibial insert surface in a proximal view at the same flexion angles as those measured in Fig. 5. The red area where proximity is within the 0.5 mm threshold was given as the virtual contact region, and the region values on both medial and lateral surfaces at each flexion angle are listed in Table 3. Anteroposterior translation of contact center for each flexion angle is listed in Table 4. Although the virtual contact region on the insert surface was observed to lie within 0.5 mm, we could easily understand the location and translation of the region during deep knee flexion. In addition, the contact of the “post” of the tibial insert as well as that of the medial and lateral surfaces was detected (Fig. 6c–e).

Table 4

Anteroposterior translation of contact center on the medial and lateral surfaces of the tibial insert at flexion angles of (a) 0.0°, (b) 31.9°, (c) 66.4°, (d) 87.8°, and (e) 110.7°

Medial/lateral	Anteroposterior translation	Knee flexion angles (°)				
		0.0	31.9	66.4	87.8	110.7
Medial surface	Anteroposterior (x _t) (mm)	-1.3	-2.6	-1.8	-1.1	-12.3
Lateral surface	Anteroposterior (x _t) (mm)	-0.7	-4.2	-12.8	-16.6	-20.3

In clinical application, none of the pose estimations had large mismatches or gross error, and final registration was always obtained in less than 30 s. In addition, computation time of visualization of the femorotibial contact was only a few seconds for each pose due to the use of a distance volume map.

4. Discussion and conclusion

This paper presented a visualization technique of the femorotibial contact in fixed-bearing TKA using X-ray fluoroscopy, and the application to a TKA patient during dynamic motion. For long-life durability and high activity of TKA implants, observing the contact of a tibial insert is highly valuable, together with measurement of motion parameters between femoral and tibial component. If the femorotibial contact after TKA can be easily assessed under in vivo conditions, particularly under dynamic loaded conditions, it is possible to better understand the relationship between knee kinematics and articular shape, and to improve implant design or surgical strategies. For evaluation of the femorotibial contact in TKA, several techniques have been employed, including finite element modeling [3] and recording systems using pressure sensitive film or digital tactile sensors [4,5]. However, these methodologies are limited because they are only able to operate under static or quasi-dynamic conditions, and cannot be physically applied to TKA patients under dynamic in vivo conditions.

For visualization of femorotibial contact, the proximity between surfaces of femoral component and tibial insert was calculated, and mapped onto the insert surface model. This technique has already been applied to analyze inter-bone distances in the field of static kinematics for the normal knee joints using MRI [15]. In our study, the region for which the tibial insert surface was found to be within 0.5 mm from the femoral component surface was designated as the virtual contact region (red area in Fig. 6), because contact between the two components contributed to the relative pose estimation accuracy, particularly the accuracy of longitudinal (y-axis) translation (rms error of 0.31 mm in Table 1). As reference data, the contact areas of the same type of

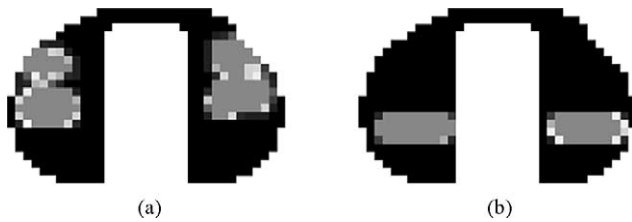


Fig. 7. Representation of the contact areas of knee implants using a digital tactile sensing system. The same type implant used in this study was tested. The total values for the contact areas at flexion angles of (a) 0° and (b) 90° were 408 and 140 mm^2 , respectively.

implants determined using a digital tactile sensing system (K-scan; Nitta Corporation, Japan; Teckscan Ltd., South Boston, USA) are shown in Fig. 7. The implants were loaded at 2000 N and tested at flexion angles of 0 and 90° . The total contact areas for each flexion angle were then found to be 408 and 140 mm^2 , respectively. When compared to the contact areas shown in Fig. 7, the virtual contact regions determined using our technique did not differ greatly (red area in Fig. 6). Although the virtual contact regions were displayed with jagged shape, this may have been caused by using polygonal model data of knee implant that do not have a smooth curved surface. On the other hand, for quantitative data (Table 3), our technique might give an overestimation of the contact region due to its proximity threshold. However, the obtained data can be considered useful to assess changes over time in the location and size of the contact region during dynamic motion.

In comparison with the motion parameter values listed in Table 2, the serial data shown in Fig. 6 also enables us to analyze the translation of the medial and lateral condyles of the femoral component, in conjunction with data for internal/external rotation. In quantitative analyses, as shown in Table 3, the virtual contact region of the tibial insert surface decreased as the knee flexed. This means that the femoral component was gradually approaching the edge of the tibial insert, and conformity between the two components was reduced. As knee flexion was reached a maximum, virtual contact on the medial surface was not observed (Fig. 6e). This phenomenon is called femoral condylar liftoff and can be explained by the increased abduction angle, as shown in Table 2. Furthermore, it is interesting to note the contact of the “post” of the tibial insert as well as that of the medial and lateral surfaces (Fig. 6c–e). The “post” functionally acts as a substitute for the posterior cruciate ligament. Therefore, detection of this “post” is valuable in evaluating the contact mechanics during dynamic motion for patients with posterior stabilized TKA. Table 4 revealed that the contact center moved in the anteroposterior direction during flexion. By bending in that way, the posterior translation on the lateral side was larger than that on the medial side, reflecting the external rotation of the femoral component shown in Table 2.

Visualization and measurement of the femorotibial contact or its region by the present technique resulted in some error, such as in pose estimation accuracy and proximity

threshold. Therefore, complete data is not always obtained. However, this technique enabled us to better understand or predict the location, translation and size of the contact region during dynamic motion. This type of evaluation can be helpful for improving implant design and optimizing TKA surgical techniques. Improvements of the present technique and validation of overall accuracy are tasks that should be dealt with a subsequent study.

Acknowledgements

The authors would like to thank Stryker Howmedica Osteonics Corporation for providing the CAD models of knee prosthesis.

References

- [1] Bartel DL, Bickness VL, Wright TM. The effect of conformity, thickness, and material stresses in UHMWPE components for total joint replacement. *J Bone Joint Surg* 1989;68(A):1041–51.
- [2] Wright TM, Rimnac CM, Stulberg SD. Wear of polyethylene in total joint replacement. Observations from retrieved PCA knee implants. *Clin Orthop* 1992;276:126–34.
- [3] Morra EA, Postak PD, Plaxton NA, Greenwald AS. The effects of external torque on polyethylene tibial insert damage patterns. *Clin Orthop* 2003;410:90–100.
- [4] Szivek JA, Anderson PL, Benjamin JB. Average and peak contact stress distribution evaluation of total knee arthroplasties. *J Arthroplasty* 1996;11:952–63.
- [5] Harris ML, Morberg P, Bruce WJM, Walsh WR. An improved method for measuring tibiofemoral contact areas in total knee arthroplasty: a comparison of k-scan sensor and fuji film. *J Biomech* 1999;32:951–8.
- [6] Banks SA, Hodge WA. Accurate measurement of three-dimensional knee replacement kinematics using single-plane fluoroscopy. *IEEE Trans Biomed Eng* 1996;43:638–49.
- [7] Hoff WA, Komistek RD, Dennis DA, Gabriel SM, Walker SA. Three-dimensional determination of femoral-tibial contact positions under *in-vivo* conditions using fluoroscopy. *Clin Biomech* 1998;13:455–72.
- [8] Zuffi S, Leardini A, Catani F, Fantozzi S, Cappello A. A model-based method for the reconstruction of total knee replacement kinematics. *IEEE Trans Med Imag* 1999;18:981–91.
- [9] Haneishi H, Yagihashi Y, Miyake Y. A new method for distortion correction of electronic endoscope images. *IEEE Trans Med Imag* 1995;14:548–55.
- [10] Weng J, Cohen P, Herniou M. Camera calibration with distortion models and accuracy evaluation. *IEEE Trans Pattern Anal Machine Intell* 1992;14:965–80.
- [11] Kozinska D, Tretiak OJ, Nissanov J, Ozturk C. Multidimensional alignment using the Euclidean distance transform. *Graphic Models Image Process* 1997;59:373–87.
- [12] Luenberger DG. *Linear and nonlinear programming*. Reading, MA: Addison Wesley; 1984.
- [13] Grood ES, Suntay WJ. A joint coordinate system for the clinical description of three-dimensional motions: application to the knee. *J Biomech Eng* 1983;15:136–44.
- [14] Schroeder W, Martin K, Lorensen B. *The visualization toolkit: an object-oriented approach to 3-D graphics*. Englewood Cliffs, NJ: Prentice-Hall; 1996.
- [15] Cohen ZA, McCarthy DM, Kwak SD. Knee cartilage topography, thickness, and contact areas from MRI: *in-vitro* calibration and *in-vivo* measurements. *Osteoarthritis Cart* 1999;7:95–109.